VOL. 15, NO. 16, AUGUST 2020 ISSN 1819-6608
ARPN Journal of Engineering and Applied Sciences

www.arpnjournals.com

CHARACTERIZATION AND SIMULATION OF APERIODIC NOISE GENERATED BY LINEAL AND NON-LINEAR LOADS IN A RESIDENTIAL-TYPE ELECTRIC SYSTEM BASED ON THE MIDLENTON MODEL

Pablo Emilio Rozo Garcia, Johann Alexander Hernández Mora and Francisco Santamaria Piedrahita
Doctorate in Engineering, Faculty of Engineering, University District Francisco José de Caldas, Bogotá, Colombia
E-Mail: perozog@udistrital.edu.co

ABSTRACT

In this work, the asynchronous impulsive noise present in electric lines is characterized. This noise is used as communications media -PLC- which is stochastic by nature and turns detection into a complex matter. In first place, it is determined how to carry out the detection of aperiodical noise and the conditions in which it must be detected and the measuring environment, the selection of linear and non-linear loads and the measuring equipment are also discussed. The algorithms used to process the information are also implemented. The detected impulsive noises are Burst type since they are the most critical in an electric line communication system. Said noises were predicted using statistical processes and characterized using the Middleton model. A proposal was stated to detected aperiodic noise and, hence, a testing system was implemented in a household with several appliances in different states such as connection, disconnection, turn on, turn off, etc. The results are favorable and two types of aperiodic noise were found: type 1, whose first impulse is high but is diluted over time and the Burst type that corresponds to an oscillation with a specific frequency which is maintained during a period of time as indicated in the classification of aperiodic noise.

Keywords: impulsive noise, middleton model, power line communication, algorithms, burst, noise simulation.

INTRODUCTION

Communications have been one of the most important areas all over the world and the one that has evolved the most over the last decades [1]. Twisted pair technologies, coaxial cables, optic fibers, microwaves, satellite waves and wireless systems have all been explored. Although PLC - Power Line Communications - rose a long time ago and their use was limited to certain applications in companies that generate and distribute energy, they are now being broadened to applications that require high frequency levels such as smart homes based on IoT (Internet of Things), follow-up and inventory management of assets, transportation, vending machine services, smart grids, industrial automation, agriculture / cattle raising, medicine and sports [2].

Communication through electric lines has been studied since it can minimize costs [3], [4], [5] by using the infrastructure of the electric system. Every building has access to it and it requires little investment to establish the transmission of data [6], [7], [8]. However, the main drawback of this technology are the generated noises, through the environment or the nature of the transmission media [9], [10], [11]. The noise in power lines is classified into background noise, narrow band noise and impulsive noise, with the last one being the most inconvenient [12], [13], [14]. Impulsive noise is divided into periodic (synchronous and asynchronous) noise and aperiodic noise which is more critical given its presence high spectral density commuting equipment [12], [15], [16]. This document focuses in aperiodic or asynchronous noise, where it needs to be sensed, understood and analyzed mathematically in order to characterize it. It is necessary to determine the parameters, characteristics and conditions in which it may present itself [17], [18]. This type of noise, due to its statistical processes and parameters, can be analyzed with methods from Poisson, Markov and Gauss [19], [20], [21], [22]. Once the statistical process has been reviewed, a technique is used to model aperiodic noise using Bernoulli-Gauss, Poisson-Gauss and Middleton models [23], [24], [25], [26], [27], [28], [29]. In this article, two detection methods for this type of noise are presented with linear and non-linear loads. Different tests are carried out with several appliances in real conditions within a residential network and the Middleton method is used to characterize the aperiodic noise including the Burst type.

Given that the three aspects that have an impact in the efficiency of a communications system are the attenuation, the variation of impedances throughout the channels and the noise, some studies have been made on these aspects. Sabih et al. in [35] carry out a study focused on noise which uses an anechoic camera that isolates a space from the electromagnetic activity of the environment and rejects narrowband noise with experimental purposes. A power filter with a frequency of 30 kHz to 1 GHz is used as well as a transient limiter to counter the variations in impedance. An Agilent spectrum analyzer is used as a measuring element to determine the characteristics of the noise during testing. Figure 1 shows the experiment settings. The model focuses on impulsive periodic noise so the analysis was eased through a cyclical stationary process, showing the self-relationship of the absolute value of noise waveform during a single period of the alternative current cycle.

In the mathematical analysis, the Power Spectral Density (PSD) delivers a noise frequency which can be related through the Fast Fourier Transform (FFT) with the self-relation function which proves that this type of noise

is cyclostationary. This enables to quantify the parameters of maximum excursion (Pe) and maximum power change during an alternative current cycle (Tr). The desktop computer and the drill were determined to cause higher periodic noise.

$$Pe = \max\{10\log_{10}[S_{N_{KM}}(t,f)]\} - \min\{10\log_{10}[S_{N_{KM}}(t,f)]\} \quad (1)$$

$$Rc = \max\{|10\log_{10}[S_{N_{KM}}(t+T_r,f)] - 10\log_{10}[S_{N_{KM}}(t,f)]|\} \quad (2)$$

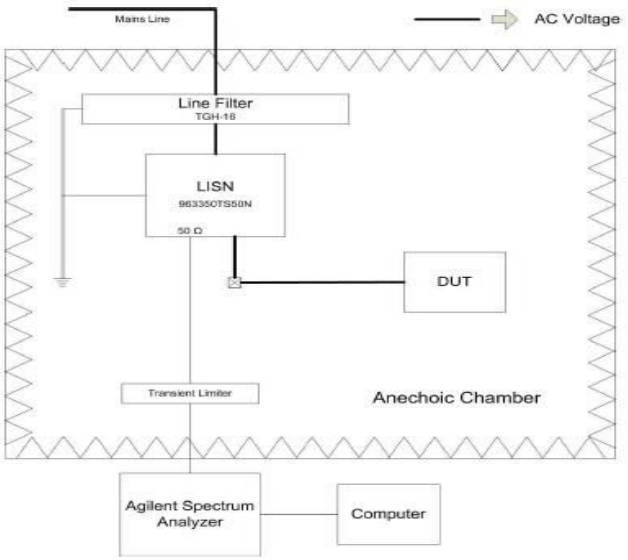

Figure-1. Description of the measurement process [35].

In [36], Cañete carries out a study on the viability of electric installations in domestic settings or small offices for high-speed data transmission within LAN networks. Hence, its behavior was modeled as a channel or a processing system of communication signals. Although the studies involved real loads in a residential and office network during connection and disconnection moments, the author centered his work in the characteristics of the transmission media based on the load variations that lead to variations in network impedances. This work considered stationary and cyclostationary noise in order to model the channel, it was not concerned on attenuating noise and the non-stationary noise was not considered given its random presence. The author proposes a communication channel model, where the simulations determined that this communication strategy is a viable alternative.

The author states that his work needs to be continued by extracting statistical values of the channel parameters such as the noise over the channel and separating the stationary noise with the non-stationary impulsive noise. The focus of the present research seeks to characterize this type of noise to eventually propose a device that can improve the efficiency of transmission information in another article.

In [37], Crallet et al. study the factors that influence the design of a BPLC (Broadband Power Line Communications) system within households for internet access, using the channel model proposed by Anatory *et al.* [38] where the distances between the distribution transformer are considered as well as the transversal section of the conductors and their distances to different circuits. Crallet uses an OFDM system based on BPSK to calculate the number of subcarriers that are required to maintain an active communication depending on the channel impedance and the SNR average.

DESCRIPTION

This work focused on the noise the present in the electric lines when they are used as a communication channel. As previously stated, there are five types of noise in PLC systems, where the most critical is the impulsive aperiodic (or non-stationary) noise due to its strong stochastic behavior. This noise leads to a high degree of inefficiency in the channel which puts the interest on characterizing it under different conditions and at its origin, given that its generation depends directly on the load.

At first, linear loads which are traditionally used in residential environments were classified (computers, X-box console, microcontrolled laundry machine, etc.). Due to their randomness, the conditions in which they present themselves must be determined which is why test were carried out in the connection, disconnection, turning on and off stages. It is necessary to place a high-pass filter over the electric grid that can capture the noise caused by the respective loads.

A RIGOL oscilloscope was used as a measuring element with the characteristics needed to capture noise, incuding a large number of samples per measurement, and then create a .CSV file which is processed in MATLAB to reproduce the noise generated by the load. The FFT was applied due to its behavior to reproduce the captured sample. This reproduction can recreate the real signal and derive from it a characterization of aperiodic or non-stationary noise over the communication channel of a PLC system.

In order to model the aperiodic noise, the Middleton method is used based on the research from Texas University, that determines the moments from the values of the impulsive index A and the impulsive parameter K. A statistical process in the data allowed to obtain the values that could recreate the aperiodic noises caused by the linear and non-linear loads.

The results obtained enabled to determine a group of three types of aperiodic noise; the non-stationary type which is present in both linear and non-linear loads and the Burst type which is only present in linear loads. Using statistical tools, all three types of noises were recreated with high accuracy and this allowed to characterize aperiodic impulsive noise. Some interesting conclusions are obtained which lead to propose some alternatives that can mitigate this type of noise in a future article in order to improve the efficiency of this communication channel.

EXPERIMENTAL SETTINGS

Physical Process

The implemented settings of this work involved real conditons in different residential homes in the socio-economic strata 3 and 4. In all cases, everyday environments were set that included all natural disturbances of the communication channel, the noises of the environment and specially the aperiodic noise caused by linear and non-linear charges in an electric grid of 115 Vrms and 60 Hz. In order to sense aperiodic noise, the block diagram in Figure 2 was implemented where a power strip was connected to the electric grid in order to hook the previously chosen linear and non-linear load(s). The filter is also connected to capture noise and an oscilloscope is used to register and display the data.

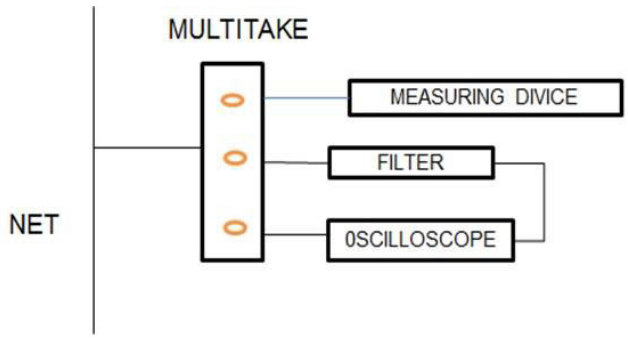

Figure-2. Block diagram for the metering process.

Implementation and Settings

Given that the behavior of linear and non-linear loads is not the same, it was necessary to classify said loads and apply the experiment under different conditions, i.e. four measurements were made for each noise generator and the significant data was registered:

- Connection to the power strip
- Disconnection to the power strip
- Turning on the equipment
- Turning off the equipment

Given that the main frequency of the network should be eliminated as well as its closest harmonic pairs (information of interest is over 1 kHz), a high-pass filter was designed and implemented.

For the detection of aperiodic noise with linear loads, a passive filter was used as seen in Figure-3. It does not polarization and has large bandwidth. The use of a second order high-pass filter was stated for the network frequency elimination stage.

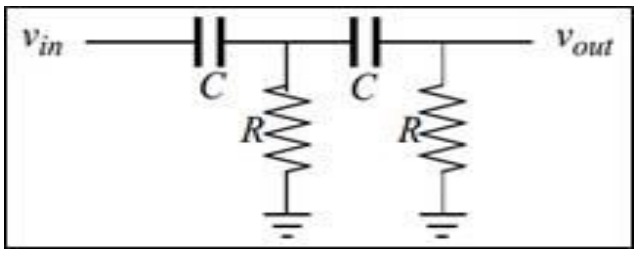

Figure-3. Second order high-pass filter comprised of two first order filters in cascade.

In the case of the aperiodic noise with non-linear loads, an active fourth order Butterworth filter was used as seen in Figure-4, in order to reject enough frequencies under 1 KHz and obtain high selectivity.

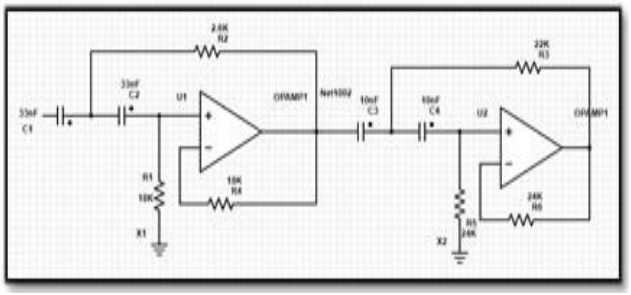

Figure-4. Esquema filtro pasa alto de cuarto orden compuesto de dos filtros de segundo orden en cascada.

Nonetheless, it was determined that the most effective method to sense aperiodic noise comprise active filters, since the external noises such as background and narrow band noises are reduced due to their smaller proportions, signal losses or attenuations are null and offer a certain gain.

For measurements, the oscilloscope was set to be activated only when a rise flank of over $50V/\mu S$ is detected. This guarantees that only the impulsive events are considered. The oscilloscopes used for measurements are RIGOL DS-1052E and Agilent MSOX3104A for linear and non-linear loads respectively, which were defined as follows:

- The filter output was connected to channel 1 through a direct probe (without attenuation) in a scale from 2 to 10 V.
- The network frequency was connected to channel 2 through an attenuated probe (10 ×) in a 10 V scale.
- The trigger mode is set in slope mode with reference to the ground. The slope varies from 1V / μS up to 50V / μS depending on the duration of the impulse (variable for any equipment).
- The screen sweep was set to vary between 500 µs and 5 ms so that the generated impulses (isolated or burst-type) could be recorded.
- A USB unit was used to store samples, the storage depth is defined at maximum level, managing to store 8120 samples per measurement in a CSV format, from

which the last 4000 are registered after the trigger is shot.

Furthermore, the measurement process is described. The visualization of the obtained in the oscilloscope was carried out through the elaboration of an algorithm in Matlab - Figure-5 - that reads the CSV file and creates a figure for information display. Hence, the corresponding parameters can be recorded.

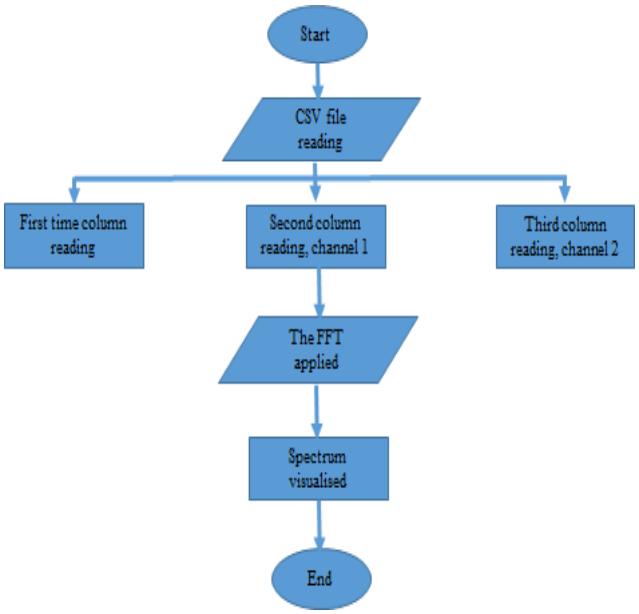

Figure-5. Flow diagram of the algorithm used to display data obtained during testing.

The Middleton method was used to characterize the aperiodic impulsive noise. The method used to estimate the parameters A, K and the Middleton model were based on [24] by following these steps (Figure-6):

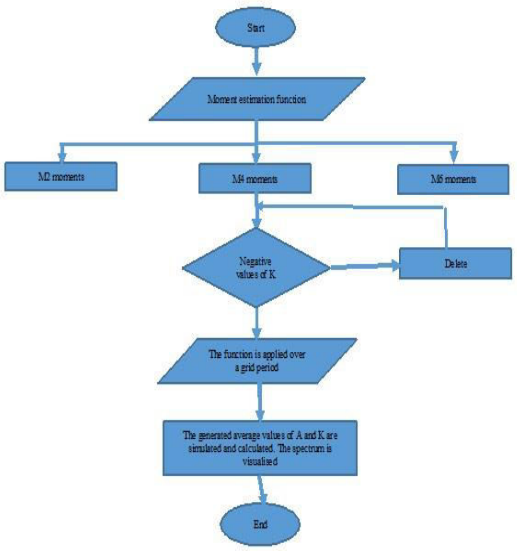

Figure-6. Flow diagram of the procedure used to determine A and K of the Middleton model.

Generation of Samples [12]

The algorithm developed in [25] was used to generate impulsive noise samples and is convenient for impulsive noise of type 1. For the burst-type noise, a special treatment was required. The algorithm consists of four main actions where the main goal is to implement the equation of the Middleton model which is completely discussed in [12], where the equation is restricted to the number of terms of the density function, specified by a predefined parameter. The flow diagram of the algorithm is shown in Figure-7.

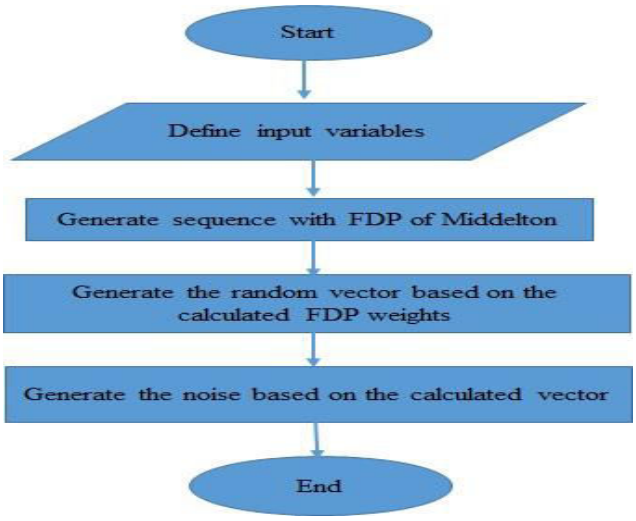

Figure-7. Flow diagram of the sample generation algorithm.

Each stage is now described.

Define input-type variables. The Middleton model requires four input parameters:

A: Impuslive index.
K: Impulsive parameter,
N: Number of terms of the equation

$$F_M(n_K) = \sum_{m=0}^{\infty} P_m N(n_k, 0, \sigma_m^2) \quad (3)$$

M: Number of samples that are generated. A vector with 1000 samples is usually generated.

Generate a sequence with a probability density function fitted to the Middleton model. In this stage, the weight vector is defined (the function calculated for each point) where the terms are computed based on the Middleton function:

$$Pdf = E^{-A} * A^{\frac{M}{!M}} \quad (4)$$

Where vector M is the vector of length M in steps of 1.

Generate a random vector based on the weight vector. In this sequence, the "SelectionMat" with the radnsample function, that takes a random sample by replacing it in all the terms of the vector length.

If the position i of the vector is equal to the jth iteration in the cycle, then the noise data in this position is derived by the jth term of the sum of the Class A Middleton probability function where the variance is:

$$\frac{j}{A} + \frac{Gamma}{1+Gamma} \quad (5)$$

For large values of N, $\frac{j}{N}$ is approximated to $E^{-A} * A^{\frac{j}{ij}}$

Generate the noise sample based on the previously generated vector. The data in the sample are computed. Hence, a FOR cycle is used to calculate the Middleton function for each index. The *noise_data* output vector is generated by allocating the output vector, according to the computed distribution with its respective variance and mean.

Estimation of Parameters [25]

The estimation of the sample parameters was based on the same toolbox, with the *RFI_EstMethodofMoments* function. The operation of the algorithm for parameter estimation is now detailed.

For the complete characterization, the set of parameters $P_3(A_A,\ \Gamma_A', \Omega_{2A})$ must be estimated where these are obtained according to the moments of the density function given by:

$$E_a^{2k} = \frac{k!^2 2^{2k}}{(2k)!}[(-1)^k \frac{d^2k}{d\lambda^{2k}} \hat{F}_1(ia_A\lambda)] \quad (6)$$

Where k=0, 1, 2, 3 leads to:

$$E_A^{<0>} = 1 \mid E_A^{<2>} = 1 \quad (7.a)$$

$$E_A^{<4>} = \frac{\Omega_{4A}}{\Omega_{2A}^2 + (1+\Gamma_A')^2} + 2 \quad (7.b)$$

$$E_A^{<6>} = \frac{\Omega_{6A}}{\Omega_{2A}((1+\Gamma_A')^3} + \frac{9\Omega_{4A}}{\Omega_{2A}^2(1+\Gamma_A')^2} + 6 \quad (7.c)$$

The values of the global parameters are obtained through an adequate substitution of the parameter $\Omega_{2k,A}$ by an appropriate function that depends on Ω_{2A}. In this case:

$$\Omega_{2k,A} \rightarrow A_A k! \left(\frac{\Omega_{2A}}{A_A}\right)^k \quad \mid k \geq 2 \quad (8)$$

Replacing these values in equations (7.a, b, c) leads to:

$$E_A^{<2>} = 2\Omega_{2A}(1 + \Gamma_A') \quad (9.a)$$

$$E_A^{<4>} = 8\Omega_{2A}^2(\frac{1}{A_A}\ (1 + \Gamma_A')^2) \quad (9.b)$$

$$E_A^{<6>} = 48\Omega_{2A}^3(\frac{1}{A_A^2} + \frac{3(1+\Gamma_A)}{A_A} + \ (1 + \Gamma_A')^3\ ) \quad (9.c)$$

Solving for Ω_{2A}, A_A with the substitution $Z = 1 + \Gamma_A$ in (9.a) the parameters can be obtained in a simple computational manner:

$$\Omega_{2A} = \frac{3(e_4 - 2e_2^2)}{4(e_6 + 12e_2^3 - 9e_2e_{24})} \quad (10.a)$$

$$A_A = \frac{9(e_4 - 2e_2)^3}{2(e_6 + 12e_2^3 - 9e_2e_4)} \quad (10.b)$$

$$\Gamma_A' = \frac{2e_2(e_6 + 12e_2^3 - 9e_2e_4)}{3(e_4 - 2e_2^2)^2} - 1 \quad (10.c)$$

These values have to be positive (> 0) to make physical sense. These equations are implemented in a Matlab program to estimate the parameters of the samples obtained through measurements. The flow diagram of the algorithm for the calculation of the sample parameters is presented in Figure-8.

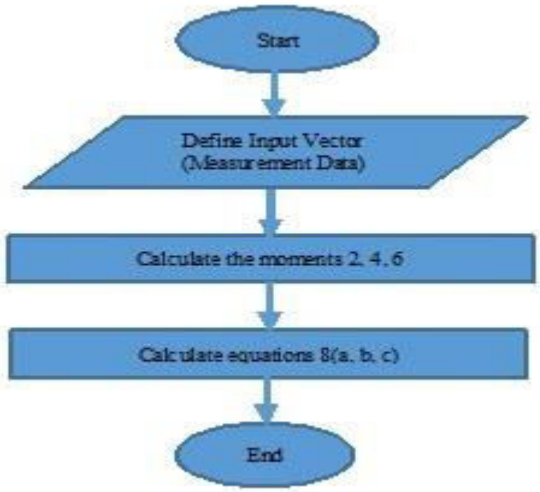

Figure-8. Flow diagram of the parameter estimation algorithm.

MEASUREMENTS

In this section, the consolidated results of the samples are shown with both linear and non-linear loads. The minimum and maximum data of **A** and **K** in each load correspond obtained after multiple samples in the statuses where aperiodic noise was generated. In each case, the histogram of frequencies where the values of **A** and **K** are presented within the samples is now shown.

MEASURING LINEAR LOADS

Table-1 presents the summary of the results recorded in different linear loads and different states.

Table-1. Specific results of the parameters A, K for all appliances with linear loads.

SUMMARY OF RESULTS					
Element	**Status**	**A (minimum)**	**A (maximum)**	**K (minimum)**	**K (maximum)**
Halogen light bulb	Turn off	0,000883940	0,048900000	0,000192590	0,157400000
	Turn on	0,001100000	0,012500000	0,001700000	0,019300000
Laptop	Without load	0,000097154	0,015900000	0,000004991	0,011500000
	Charging	0,000828000	0,004900000	0,000032245	0,002300000
Laundry machine	Connection	0,000635190	0,007900000	0,000021596	0,002200000
	Disconnection	0,002800000	0,002800000	0,000356130	0,007200000
	Turning on	0,001200000	0,019900000	0,000106330	0,059600000
	Operation (centrifuge)	0,009500000	0,050100000	0,002100000	0,054000000
Blender	Connection	0,001100000	0,011900000	0,000072823	0,009000000
	Disconnection	0,001100000	0,010200000	0,001400000	0,041800000
Microwave	Turning off	0,001000000	0,003200000	0,008600000	0,031600000
	Connection	0,000586820	0,009200000	0,000001590	0,001300000
	Disconnection	0,000591010	0,002700000	0,000049930	0,001300000
	Turning on	0,000355010	0,016300000	0,000190110	0,047700000
Motor tool	Turning off	0,002800000	0,012900000	0,001300000	0,043400000
	Connection	0,002300000	0,048800000	0,000121820	0,024600000
	Turning on	0,003500000	0,015000000	0,000500610	0,123000000
Fridge	Open door	0,002300000	0,014800000	0,000394740	0,045900000
	Close door	0,002300000	0,005100000	0,002700000	0,041600000
Ironing machine	Thermostat on/off	0,002900000	0,008900000	0,000139860	0,005700000
Television	Connection	0,003500000	0,009000000	0,000132810	0,001300000

Table-2 presents the main results of the measurements with linear loads.

Table-2. General results of parameters A and K in all appliances with linear loads

A		**K**	
Mean	**0,00886374**	**Mean**	**0,017900433**
Standard deviation	0,01254833	Standard deviation	0,033143950
Sample variance	0,00015746	Sample variance	0,001098521
Range	0,05000285	Range	0,157398410
Minimum	0,00009715	Minimum	0,000001590
Maximum	0,05010000	Maximum	0,157400000

Figure-9 presents the corresponding histograms for variables A and K where the sample distribution is depicted.

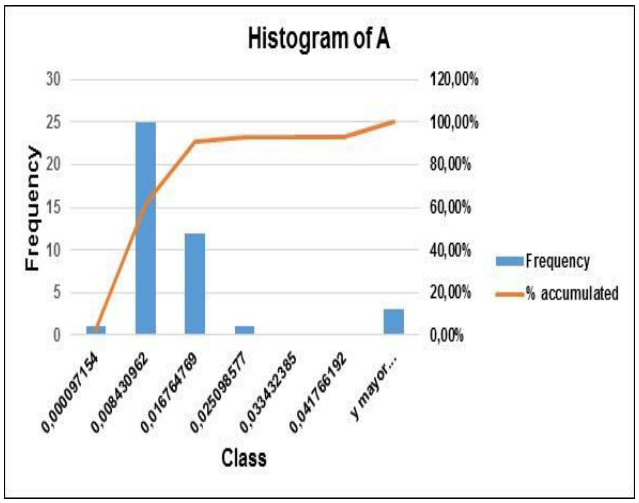

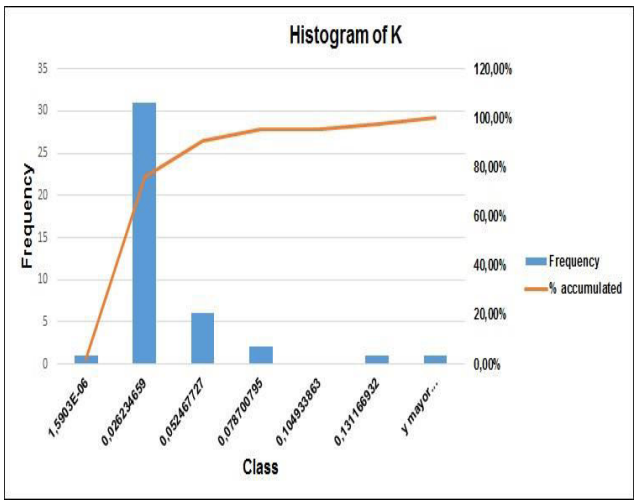

Figure-9. Histogram of variables A and K in the estimation of the parameters obtained with linear loads.

MEASURING NON-LINEAR LOADS

Table-3 summarizes the results recorded in non-linear and linear loads during different states.

Table-3. Specific results of parameters A and K for all appliances – linear loads.

Scenario	Element	Status	A	K
University	DVD	Connection	0,1976	4,0411
University	DVD	Disconnection	0,1976	4,0411
University	DC source	Connection	0,1976	4,0411
University	DC source	Disconnection	0,1990	4,0450
University	Computer	Connection	0,1990	4,045
University	Computer	Disconnection	0,1990	4,045
University	Xbox	Connection	0,2003	4,0453
University	Xbox	Disconnection	0,2002	4,0453
Household strata 3	Computer	Connection	0,2003	4,0453
Household strata 3	Computer	DIsconnection	0,2002	4,0624
Household strata 3	Microcontrolled washing machine	Connection	0,2002	4,0624
Household strata 3	Microcontrolled washing machine	DIsconnection	0,2003	4,0624
Household strata 3	Microwave	Connection	0,2016	4,0886
Household strata 3	Microwave	Disconnection	0,2016	4,0886
Household strata 3	Microcontrolled fridge	Connection	0,2016	4,0886
Household strata 3	Microcontrolled fridge	Disconnection	0,2028	4,1031
Household strata 3	Xbox	Connection	2,2028	4,1031
Household strata 3	Kbox	Disconnection	0,2028	4,1031
Household strata 4	Water source	Connection	0,2027	4,1031
Household strata 4	Water source	Disconnection	0,2027	4,1032
Household strata 4	Microcontrolled washing machine	Connection	0,2028	4,1032
Household strata 4	Microcontrolled washing machine	Disconnection	0,2124	4,1983
Household strata 4	Microcontrolled fridge	Connection	0,2124	4,1983
Household strata 4	Microcontrolled fridge	Disconnection	0,2124	4,1983
Household strata 4	Microwave	Connection	0,2133	4,2133
Household strata 4	Microwave	Disconnection	0,2123	4,2133
Household strata 4	Computer	Connection	0,2133	4,2133
Household strata 4	Computer	Disconnection	0,2126	4,2221
Household strata 4	All appliances	Connection	0,2126	4,2221
Household strata 4	All appliances	Disconnection	0,2126	4,2221

Table-4 presents the results of the measurements from non-linear loads.

Table-4. General results of parameters A and K of all appliances with non-linear loads.

A		K	
Mean	**0,2042566667**	**Mean**	**4,112236667**
Standard deviation	0,005869246755	Standard deviation	0,06969922319
Sample variance	0,0000344481	Sample variance	0,004857981713
Range	0,0157	Range	0,181
Minimum	0,1976	Minimum	4,0411
Maximum	0,2133	Maximum	4,2221

Figure-10 presents the corresponding histograms for variables A and K where the sample distribution is evidenced.

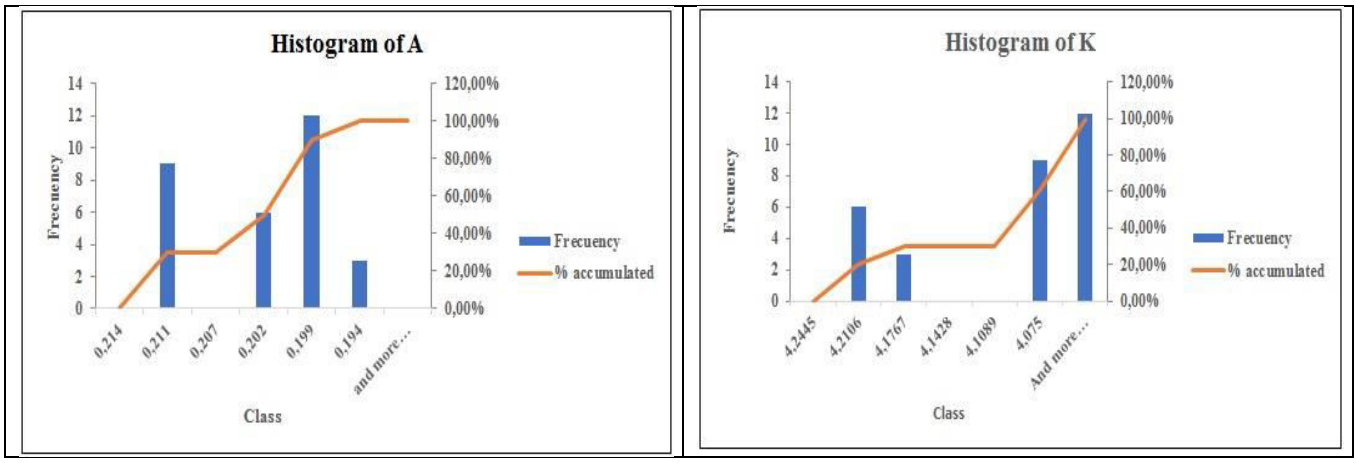

Figure-10. Histogram of variables A and K in the estimation of the parameters obtained with non-linear loads.

As seen in the measurements, in equipment with large windings or engines the connection to the multisocket generated impulses with average amplitudes between 15 to 40 V approximately, which translates into small values of A and K and a maximum background noise of 0.5 Vpp within the model. This confirms the results shown by the moment estimation algorithm.

In the measurements, two predominant behaviors were detected. The first one, known as high impulse connection, takes place in equipment with high inductive load. Only a few of these measurements correspond to pulses (no more than 5) where the value of the first impulse has peaks over 40 Vp. This impulse is characterized by its extremely short duration, where two samples of the signal correspond to 20 ns for a sampling time of 10 ns.

The second type of impulse occurs when the equipments are already under operation. In this state, they are already energized so the noise generated during state transition does not have significantly high peak values (< 20 Vp). Nonetheless, the noise itself does generate impulses so its duration is longer and is called medium level impulse long noise.

RESULTS

The measurements included several types of aperiodic noise, where the most representative are High Impulse Noise, Medium Impulse Long Noise and Burst Type Noise. In Sabih *et al.* [35], tests were carried out in laboratory conditions with an anechoic camera using a power filter with frequencies ranging between 30 kHz to 1 GHz and a transient limiter. In contrast, the tests in this work were performed in natural conditions within an electrical residential environment of socio-economic strata 3 and 4. Although the focus of both research articles is the impulsive noise, it is noteworthy to mention that the results obtained by Sabih refer to periodic impulsive noise whilst this work refers to aperiodic (non stationary) impulsive noise. On another note, since the autocorrelation function shows a periodicity in the Power Spectral Density (PSD), the cyclostationary nature of the noise generated by the devices is evidenced. The Middleton method serving as a base for this work and given the randomness of noise, the probability density function (PDF) and parameters A and K, allowed to conclude that the noise is aperiodic (non stationary) and Burst type with different characteristics depending on the devices.

An exhaustive measuring procedure was carried out for the noise incoming from different loads in real environments where the approach focused on determining the characteristics of the generated noise for each load. In contrast, the work of Cañete [36] measured noise with the purpose of modeling the channel according to the distances between the transmitter and the receiver with the

presence of the noise generated by certain loads. Anatory *et al*. [XX] determined the characteristics of noise in a real environment and went further by studying the impedances of each load in the network in order to determine the transmission power as well as the calculation of the number of subcarriers that enable internet connection without loss or attenuation of communication.

The results from this research are now described:

High Impulse Noise

It is characterized by a low value of parameters A < 0.030 and K < 0.02, where few impulses are represented (up to 5) and the maximum background noise is 0.5 Vp. To measure this parameter, the impulse connection noises were searched in the simulation results and were simulated to corroborate the proper operation of the model. Some results are displayed in Figure-11 and compared to the simulations. Figure 12 represents a zoom of the signal peak.

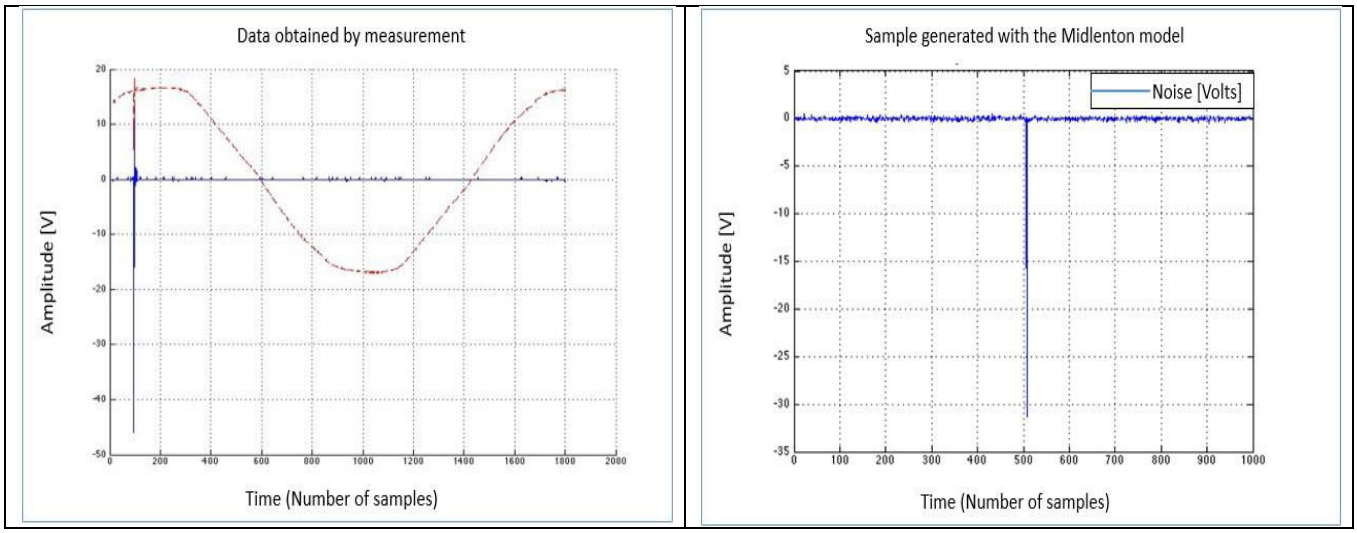

Figure-11. Left side – real measurement for the washing machine connection (measurement 8.csv), right side – real simulation with A =0,001.

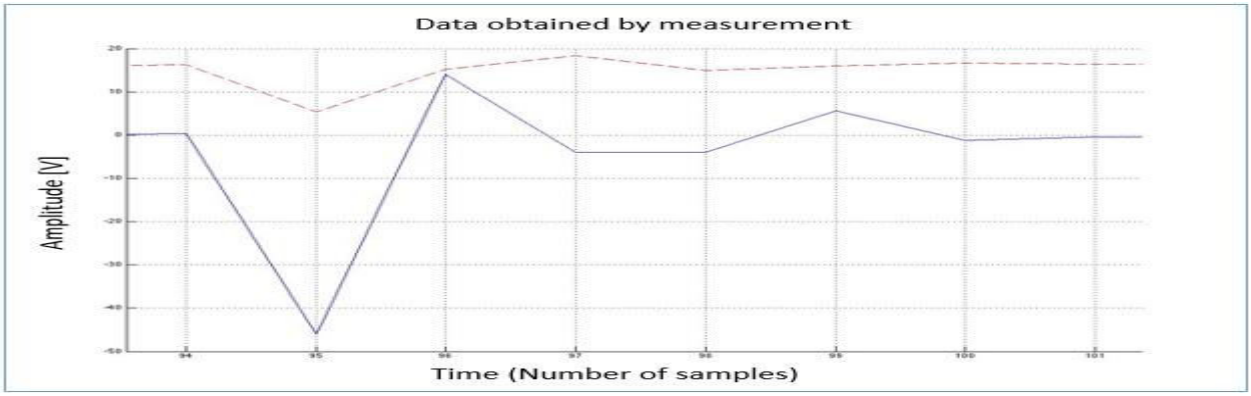

Figure-12. Zoom of the measurement with an impulse of -45V and its duration (2 samples).

Figure-13 shows a simulation for the maximum value of A (0,0030).

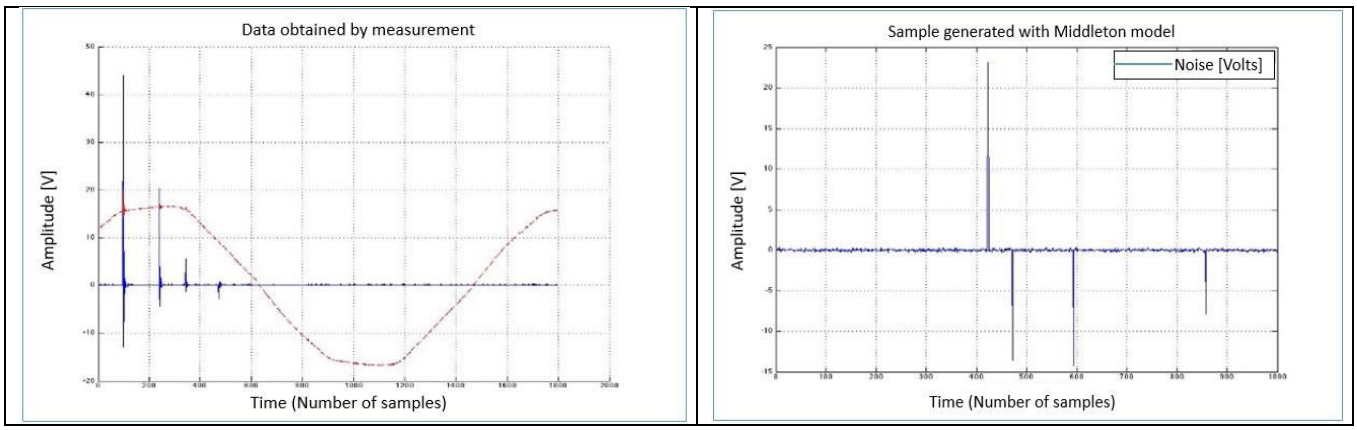

Figure-13. Left side – real measurement for the refrigerator connection (measurement 12.csv), right side – real simulation with A =0,0030.

Medium Impulse Long Noise

This type of noise is characterized by impulses that last up to half a cycle of network signal, where the amplitude of the signal can be high at any given instant, with certain lower peaks, until reaching zero. This was the case for all measurements in appliances, specially those that were already connected and were turned on / off.

The amplitude of this type of noise seldom exceeds 20 Vp and the repetitions of the impulsive event are closer to a "burst" or separated between them.

This simulation enabled to determine that parameter A for this noise is higher than 0.009 and lower than 0.2 in order to maintain the maximum background noise level of 0.5 Vpmax. Parameter K remains a constant at 0.002. Figures 14 and 15 show the results obtained in simulations and the comparison of the results.

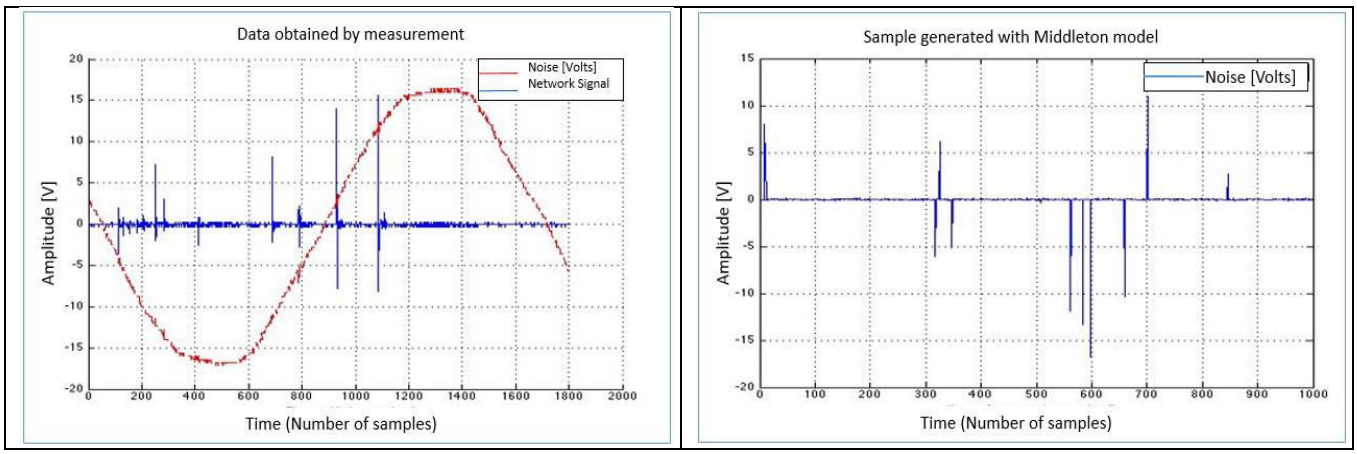

Figure-14. Left side - real measurement obtained for the connection of the laptop charger (measurement 24.csv), right side - simulation with parameter A>0.009.

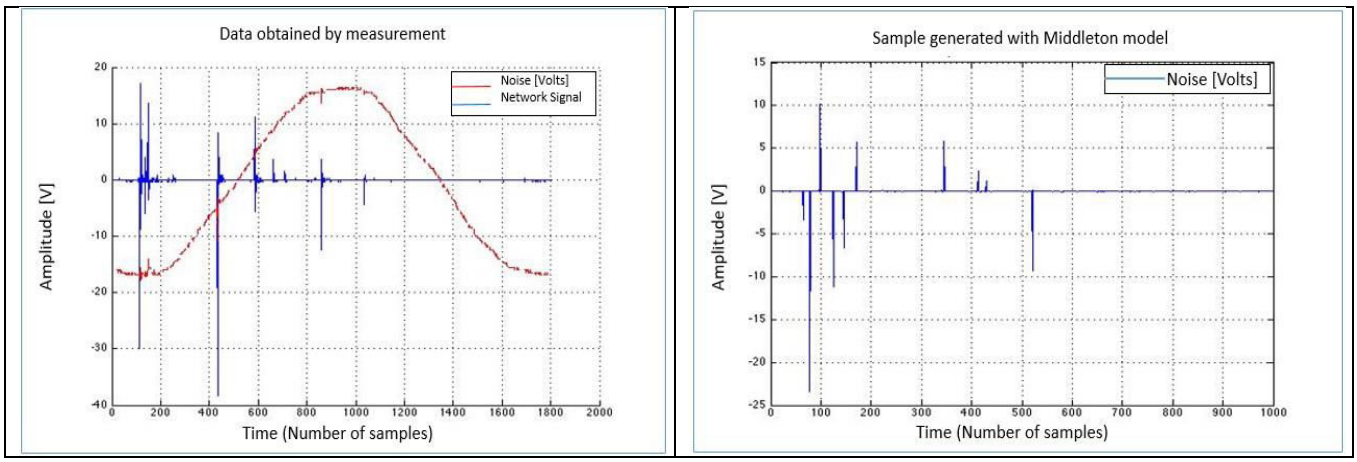

Figure-15. Left side - real measurement obtained for the connection of the laptop without charger (measurement 26.csv), right side, simulation with parameter A>0.009.

Based on the highest values of parameter A which were previously described, the sample generates more impulses in a shorter interval where the amplitude decreases to maintain the ratio between power and background noise.

Burst Type Noise

To model the burst-type noise, it was necessary to determine the average duration. The process used to determine said duration was the following:

- Out of the measurements carried out, choose the samples with more than 5 consecutive impulsive events.
- Filter the samples of background noise in order to estimate the burst duration more accurately.
- Determine the average duration of the sample.

Table-5 shows the results obtained by following the previously described procedure.

Table-5. Burst duration statistical variables.

RESULTS OF THE BURST TYPE	
Variable	**Value**
Mean	131,557143
Sample variance	10848,0184
Range	535
Minimum	15
Maximum	550
Count	70

The histogram of time values is shown in Figure-16.

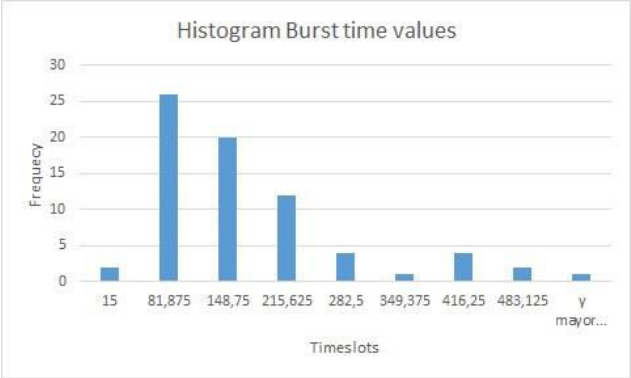

Figure-16. Histogram of burst duration.

The measurements have a longitude of 8192 samples, where the useful signal is located after the last 4000 samples. Furthermore, for a typical sample, the network cycle takes between 1600 and 2000 samples in average.

Burst Simulation

For the simulation procedure of these samples, the same algorithm of non-burst type samples was used. The difference lies in defining a time vector, in which the duration of the impulsive sample is established according to the previous table. This is combined with the first vector and thus, the impulsive sample can be obtained. The flow diagram is shown in Figure-17.

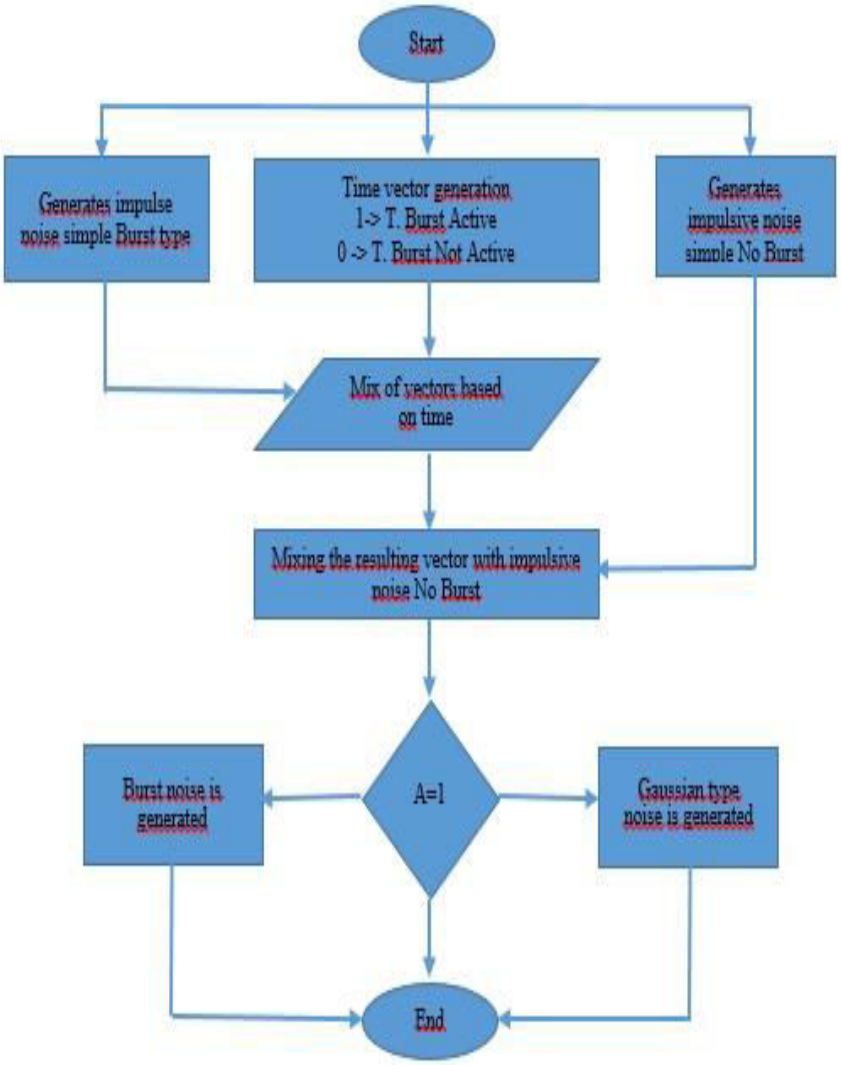

Figure-17. Algorithm for the generation of Burst-type noise (A<1) and Gaussian noise (A≥1).

The algorithm works as follows:

Generate Samples

Two samples of impulsive noise are generated: the first one is a burst type and the second one a non-burst type. The background Gaussian noise has the same parameter K for both.

Define the Burst Time Limit

A time vector is generated where the index has two possible values, 0 and 1. When the vector is equal to 1, the burst time is active and, when it is equal to 0, the burst time is already over.

Mix the Burst Vector

In this stage, the burst type vectors and the time limiter are mixed so that the samples can adapt to the measurements.

Afterwards, the resulting vector is mixed with the generated sample that is not a burst-type one. The peaks that do not belong to background noise are eliminated in the last sample, leading to the final vector.

The value of parameter A turns the sample into the Burst type and said value is 0.5 as a result of simulation. From this point, the sample generates more impulses in the time space determined for burst. Hence, its behavior goes from impulsive to Gaussian, specially after $A \geq 1$, as proven by Middleton in [22] and [24] where the complete model can be found.

In Figure-18, the results for minimum, average and maximum values of the Burst times are shown with a parameter A of 0.9 and K of 0.002, with the procedure previously described, for a typical sample duration of 1000. The sample duration may vary.

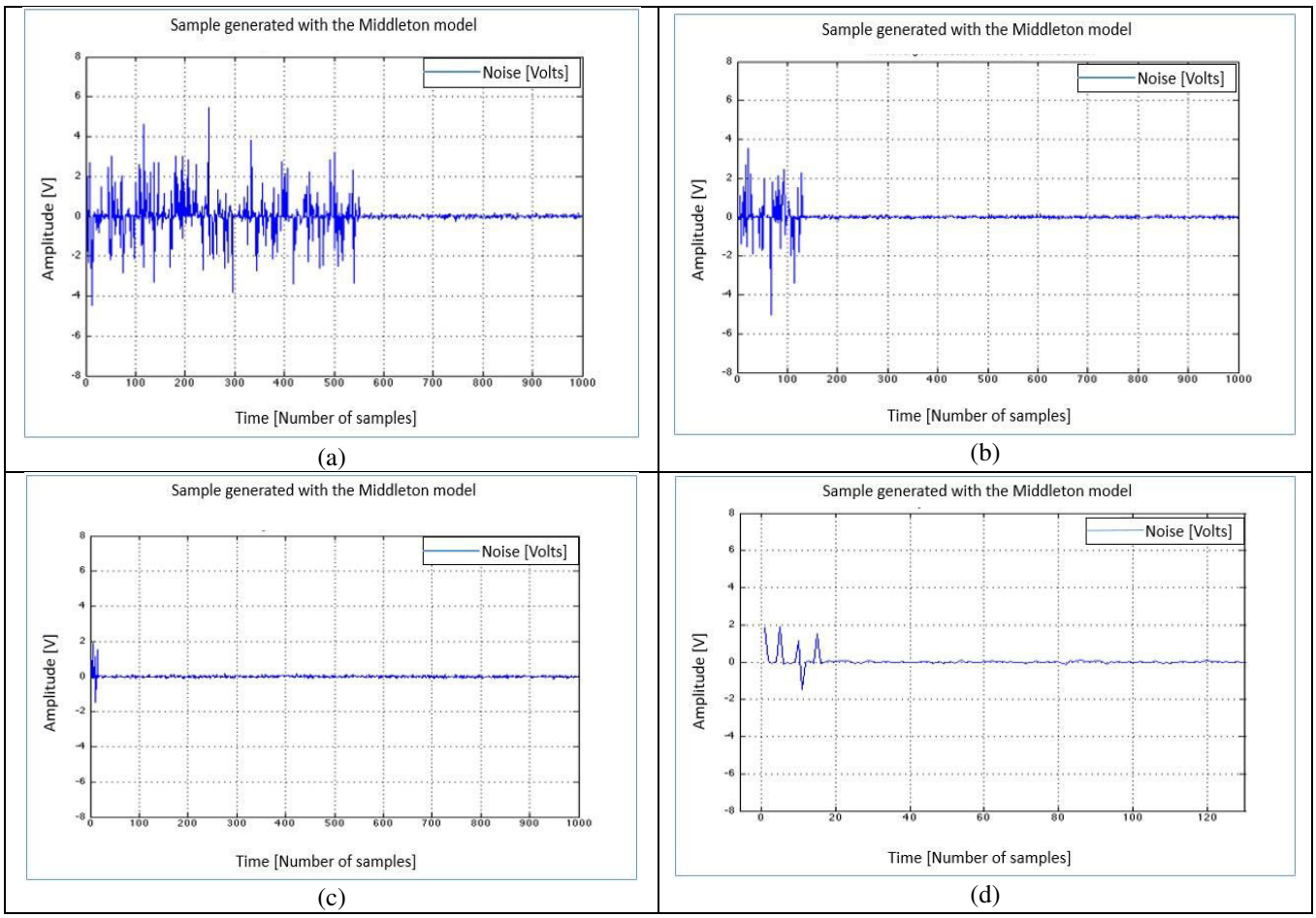

Figure-18. Burst-type impulsive noise simulations over time for A=0.5 and K=0.02 in (a) Maximum, (b) Average, (c) and Minimum times of burst (d) a zoom is made for better observation of the burst.

When parameter A is increased to 2, the sample will have more impulses during the time allocated to the Burst, as seen in Figure 19 and its behavior goes from a Poission function to a Gaussian function.

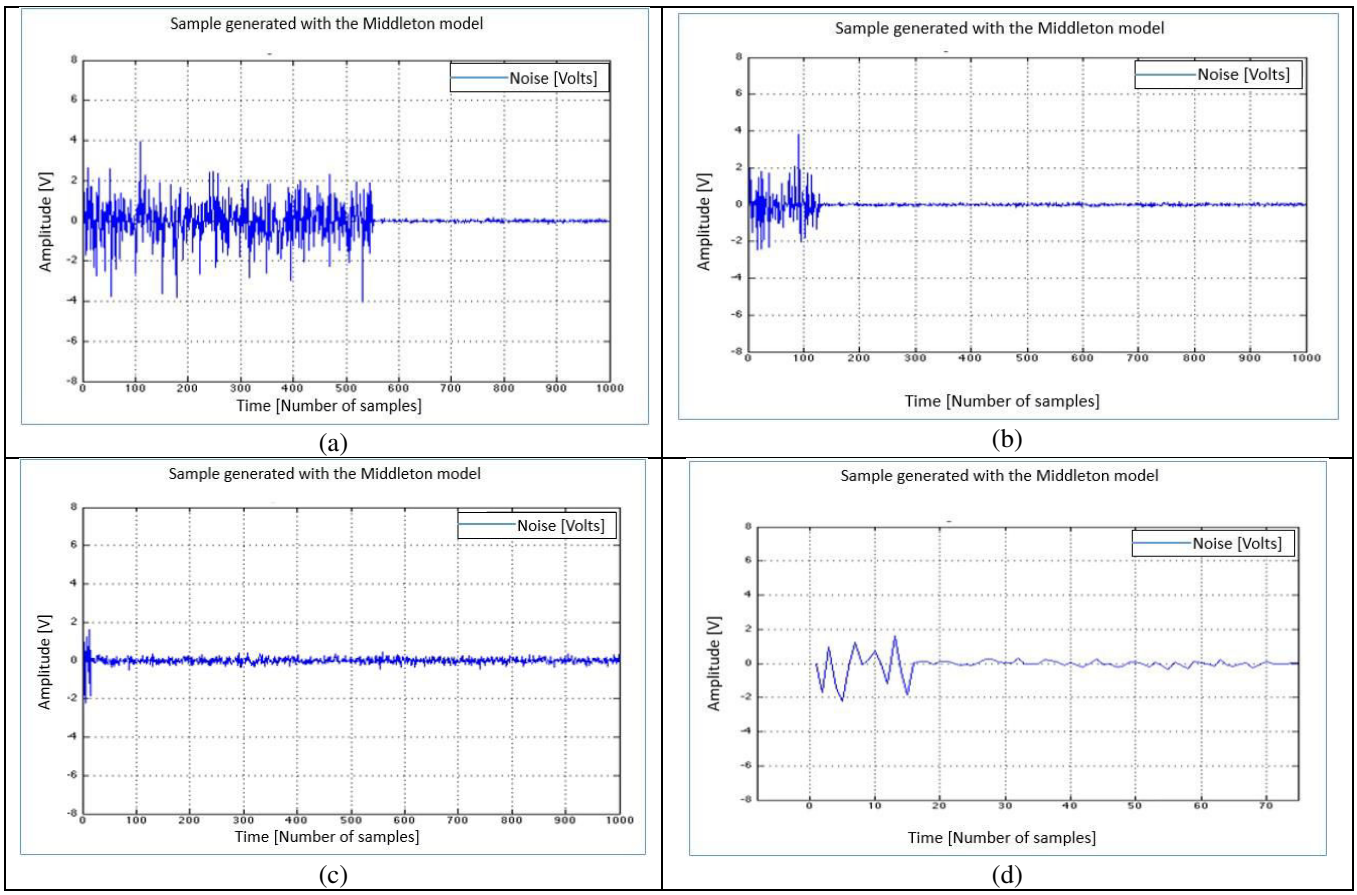

Figure-19. Burst type impulsive noise simulations over time for A=2 and K=0.02 in (a) Maximum, (b) Average, (c) and Minimum times of burst (d) a zoom is made for better observation of the burst.

Combination of Samples

Among the measurements carried out, there were samples with a burst-type behavior and once the burst was over, the samples had residual peaks throughout the network period. To model this situation, the procedure was similar than with the burst signal, except that during the combination of the vector of samples generated synthetically, the values that do not belong to background noise were not eliminated. Hence, the behavior of these two sample classes is combined. The result is shown in figures 20 and 21 for different values of A, both for the impulsive vector and the non-impulsive vector.

Average burst time and highly impulsive sample $A_{burst} = 1,\ A_{simple} = 3 * 10^{-3}$

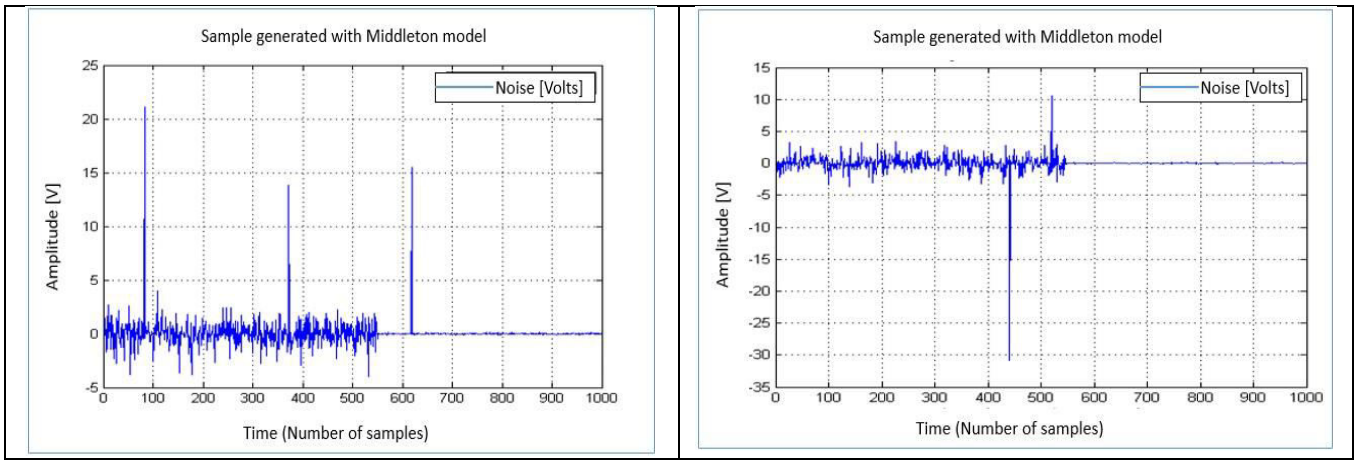

Figure-20. Simulations of combined impulsive burst noise with sporadic impulses A_{burst}=1, A_{simple}=3*10^{-3}.

Average burst time and highly impulsive sample $A_{burst} = 2,\ A_{simple} = 9 * 10^{-3}$

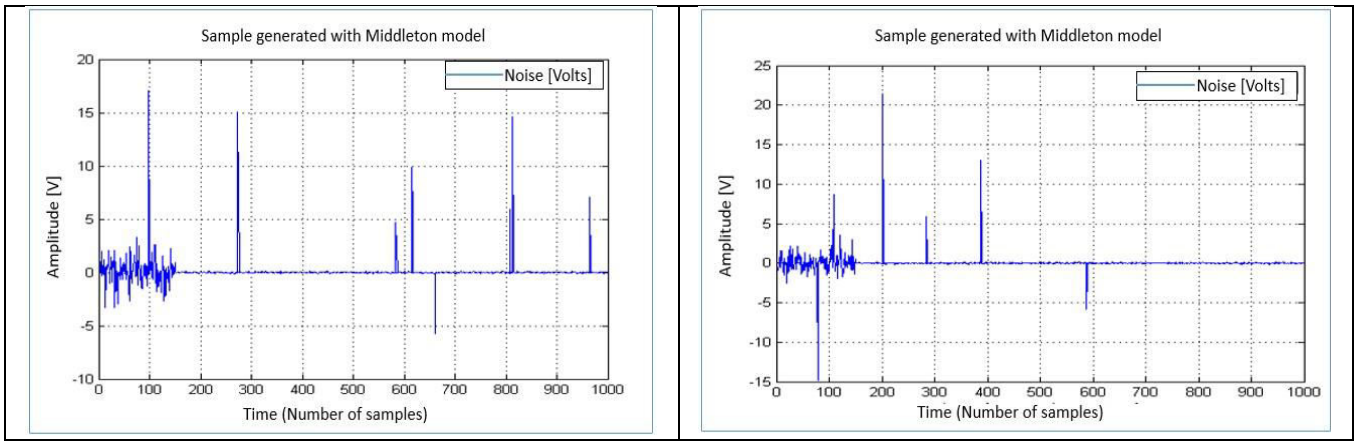

Figure-21. Simulations of combined impulsive burst noise with sporadic impulses A_{burst}=2, A_{simple}=9*10^{-3}.

As evidenced, all types of samples can be generated from real measurements based on the scripts of the Middleton model. The manipulation of these samples is quite easy. For instance, during the combined measurements of impulsive and burst signals, the impulse was conveniently chosen to be present at the beginning of the sample. However, if necessary, it could be relocated across time to either the beginning or the end of burst-type samples in the required instant. This makes the process of capturing samples more practical. Afterwards, the synthetic samples are generated and compared with the samples obtained in real measurements as seen in Figure-22.

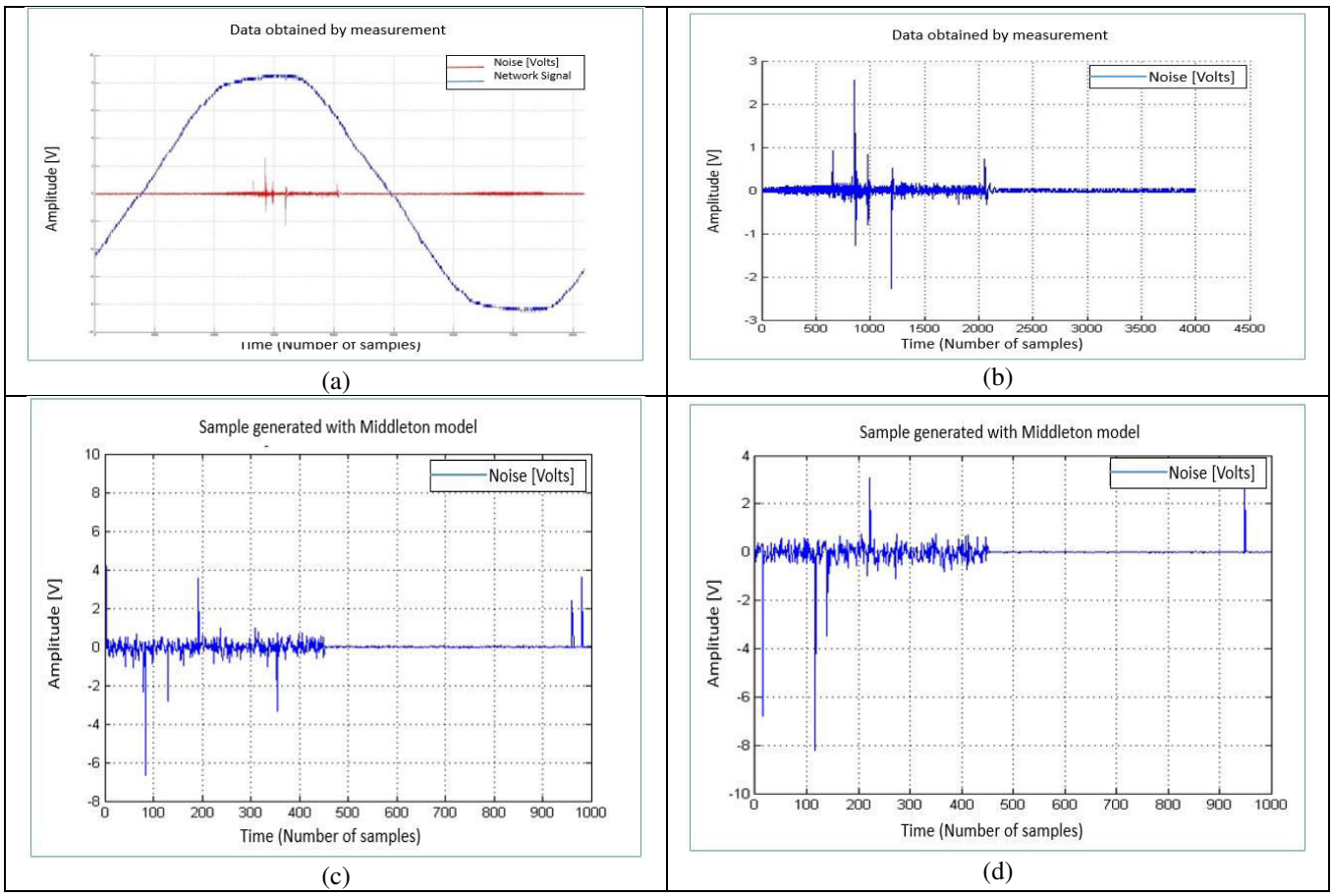

Figure-22. Comparison between the measurement of the halogen light bulb (measurement a21.csv) , (a) obtained measurement, (b) zoom on the measurement for better observation of noise (c, d) synthetic samples generated through algorithms.

The samples stored in (c,d) have the same parameters $A_{burst} = 2$, $A_{simple} = 6.9 * 10^{-3}, K = 0.002$.

There are some situations where more than one burst is present. For example, one of the measurements of the connection of the blender, there were three bursts with an approximate duration of 20 samples for the first two and 80 for the last one. In this case, thanks to the flexibility of the algorithm, a burst-type sample was generated with 1000 samples. It was then fragmented into three segments of the aforementioned duration, with the noise starting at 40, 80 and 500 samples respectively and thus representing more accurately the measurements. The result is presented in Figure-23.

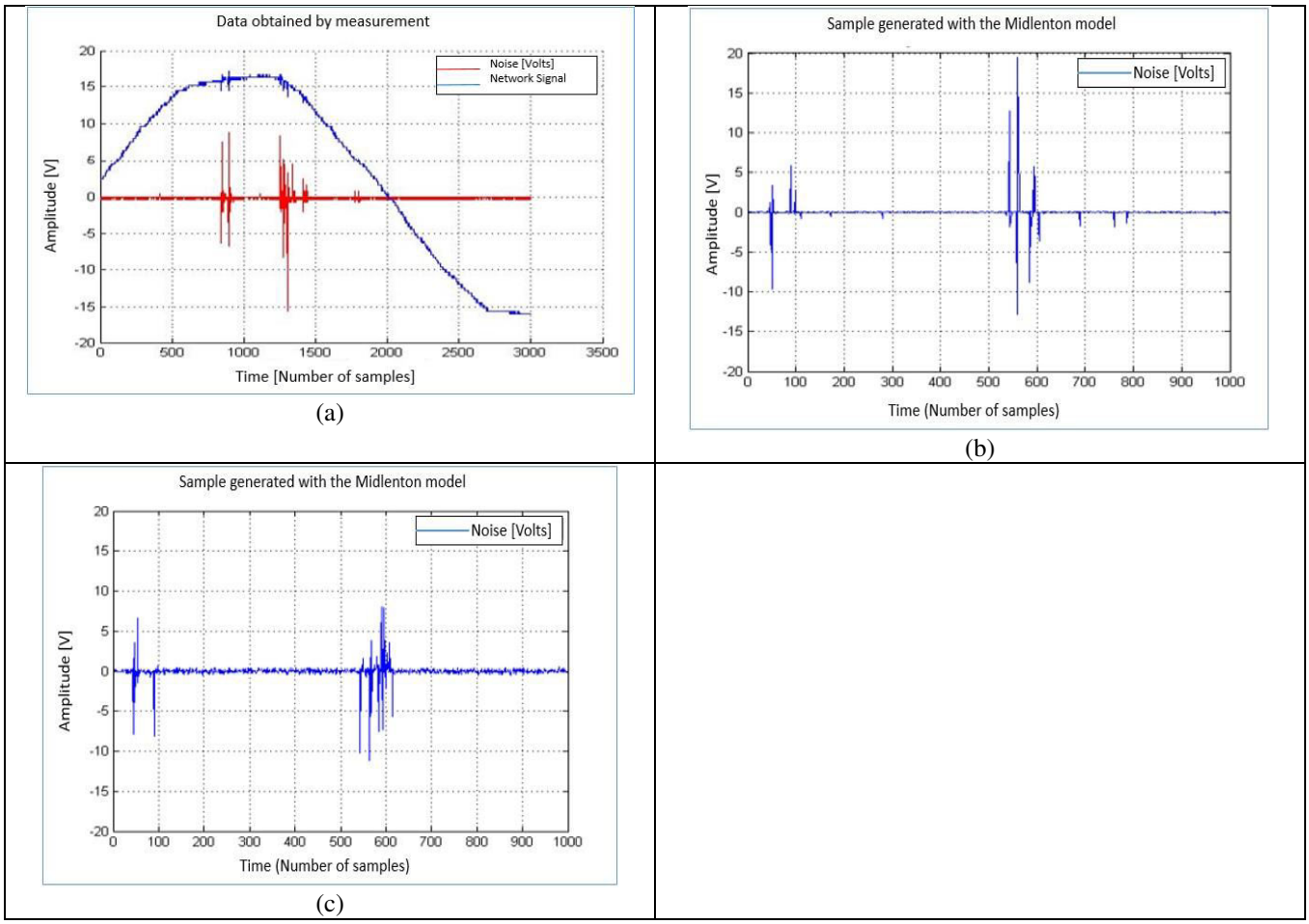

Figure-23. (a) 12th measurement of the blender, (b) n° 1 sample generated with low background noise (c) n° 2 sample with background noise of 0.5Vp

The parameters of the previous simulation were:
In (b): $A_{simple} = 6.9 * 10^{-3}, A_{burst}(0.1), K = 0.002$
In (c): $A_{simple} = 6.9 * 10^{-3}, A_{burst}(0.3), K = 0.008$

The sample is accurately represented and can be handled by adjusting the parameters A and K so that the density of impulses in the burst time can be modified as well as the background noise that reached 0.5 Vp. The amplitude and the samples can also vary. The last type of samples to be shown only appears with a long burst with high intensity in the peaks. This is the case presented in the measurements of the microwave connection, where the burst lasts 800 samples and peaks have a range of 40 Vp as seen in Figure-24.

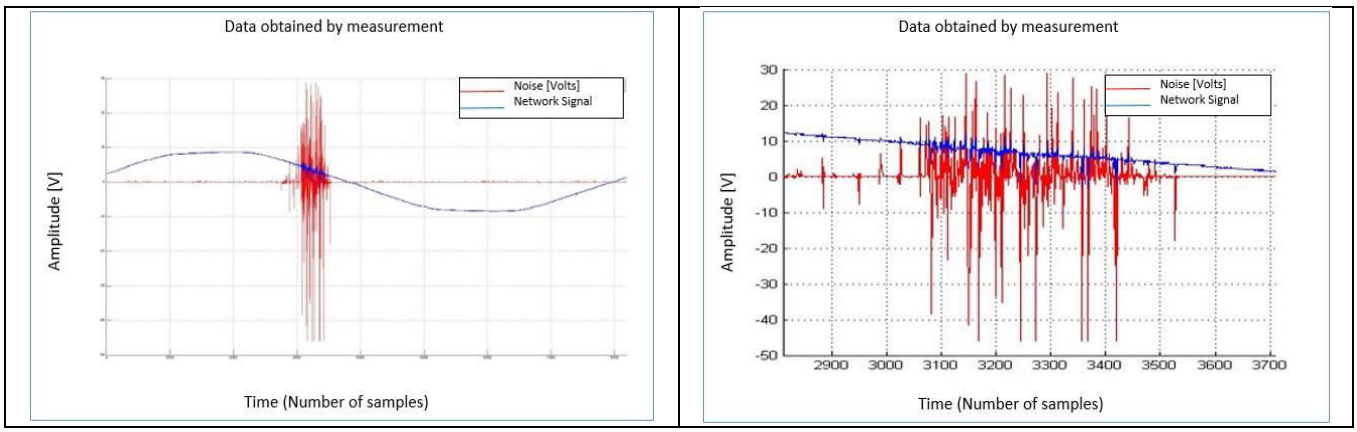

Figure-24. Measurement from microwave connection, file 11.csv, left side - complete measurement, right side - zoom.

Multiplying the amplitude by a factor of 10 in simulations, the sample is properly retrieved. 200 samples were taken as a reference out of 1000, to maintain the ratio within the measurement, which has 4000 valid samples and a noise of 800 samples. The results are shown in Figure-25.

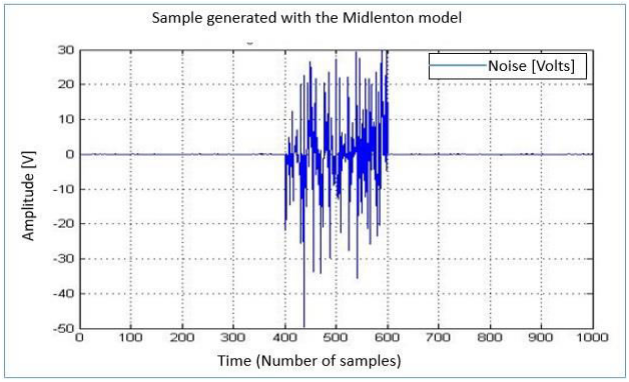

Figure-25. Simulation with parameters $A_{simple} = 6.9 * 10^{-3}$, $A_{burst} = 1$, $K = 0.002$.

CONCLUSIONS

a. With the proposed metering strategy and the implemented system, an effective and practical measurement process of the noise was achieved, including the various subclasses of impulsive noise that are present in the power network. In other work carried out to measure impulsive noise such as [21], [30] and [31], the physical properties of the channel were considered given its characterization. In the present work, the measurements were directly made at the source of the noise and not throughout the channel which simplified the identification of the main characteristics of the noise.

b. The importance of impulsive noise has been studied by different authors, from all sorts of approaches, where the statistical models are the most adequate and accurate in the behavioral prediction of this phenomenon. The Middleton model allowed to trace the noise and lead to excellent approximations due to its easy computational implementation.

c. Using easily understood algorithms (in particular those that were developed by the University of Texas [25]), the parameters that characterized impulsive noise were established. Hence, it was possible to perform a statistical analysis in which all the samples obtained from measurements were included (more than 1000 in total). The results of this analysis confirmed that the captured samples are consistent with the ranges obtained by independent studies [5], [21] amd [34]. This validates the measurements and the characterization of the impulsive noise.

d. Two subclasses of non-burst impulsive noise were identified: the high impulse connection noise and the medium impulse long noise, which were properly simulated. It is noteworthy to mention that the procedure described for the generation of burst samples enables a wide spectrum of synthetic samples, which can be adapted to the needs of interested parties. For instance, by following the tables of duration of burst and the parameters of high impulse connection noise, samples that have peaks of up to 40 V can be obtained. These samples are significant in the mitigation and study of how noise affects systems.

FUTURE WORK

The analysis using the Middleton model during simulations allowed to obtain signals close to the ones present in real conditions. Nonetheless, it would be interesting to involve other models such as the state model [17], [32] and the symmetric α-stable model (SαS), [17], [33]. These alternatives could be used in the analysis of aperiodic noise derived from the loads of an electric network. After the characterization of aperiodic noise, future work will propose how to mitigate the incidence of aperiodic noise in a communication channel through power line communication (PLC).

ACKNOWLEDGMENT

This work was possible thanks to the support of Universidad Distrital Francisco José de Caldas (Bogotá, Colombia) through the Engineering Doctorate program.

This work has also been possible thanks to the support of the Research Group LIFAE - Laboratory for the Research of Alternative Energy Sources - from Universidad Distrital Francisco José de Caldas.

REFERENCES

[1] Rehman A, Bashir N, Hassan N and Yuen C. 2016. Impact of Home Appliances on the Performance of Narrow-Band Power Line Communications for Smart Grid Applications. IEEE.

[2] [2] Mudriievskyi S. 2014. Power line Communications: State of the art in research, development and application. AEUE International Journal of Electronics and Communications AEUE - International Journal of Electronics and Communications, 68, 575-577. doi:10.1016/j.aeue.2014.04.003.

[3] Kuzlu M, Pipattanasomporn M and Rahman S. 2015. Review of Communication Technologies for Smart Homes/Building Applications. IEEE Innovative Smart Grid Technologies Conference (ISGT-ASLA), Bangkok, Thailand, November 4-6.

[4] Barmada S, Musolino A, Raugui M, Rizzo R and Tucci M. 2011. A wavelet based method for the analysis of impulsive noise due to switch communications in power line communications (PLC) systems. IEEE Transactions on Smart Grid. 2(1).

[5] Zuberi K Thesis Powerline carrier (PLC) communications system. Master of Science in Internetworking at royal institute of technology, KTH IT –Universitylet, Kista, Stockholm, Sweden.

[6] Radford D. New Spread spectrum Technologies enable low cost control applications for residencial and commercial use. Intellon Corporation.

[7] Doster Klaus. 2001. Power line communication. Prentice Hall PTR, New Jersey.

[8] Torres Maria del Pilar. Revista de derecho informatico"No. 67 febrero de 2004. Alfa Reds ISSN 1681-5726.

[9] http:// www.powerline.com.

[10] Zimmermann Manfred and Doster Klaus. 2002. Analysis and modeling of impulsive noise in broad band powerline communications. IEEE Transactions on Electromagnetic compatibility. 44(1).

[11] Hooije O. 1998. A channel model for the residential power circuit used as a digital communication medium. IEEE trans. Electromagn. Compat. 40: 331-336.

[12] Philipps H. 1999. Modeling of powerline communication channels. In Proc 3rd Int. Symp Power Line Communications and its applications. Lancaster, U:K. pp. 45-51.

[13] Husein Arslan. 2010s. Time Frecuency analysis of noise generated by electrical loads en PLC. IEEE 17th International Conference on ommunications.

[14] Zimmermann. 2000. Modeling and analysis of noise effects on broadhand power-line communications. ISPLC.

[15] Balakirsky. 2003. Modeling and analysis of noise effects on broadhand power-line communications. ISPLC.

[16] _____ 2005. Modeling and analysis of noise effects on broadhand power-line communications. Power Delivery, IEEE transacctions on. 20(2): 630-637.

[17] Corropro f, Arrabal J, Del Rio L y Muñoz J. 2006. Analysis of the cyclic short-term variation of indoor power line channels. Selected areas in communications, IEEE Journal on. 24(7): 1327-1338.

[18] Chan Morgan and Donaldson Robert. 1989. Amplitude width and interarrival distribution for noise impulse on intrabuilding poweline communications network. IEEE Transactions on Electromagnetic compatibility. 31(3).

[19] Tlich Mohamed, Chaouche Hassina, Zeddam Ahmed. 2008. Impulsive noise characterization at source. IEEE.

[20] Chaudhury Saurabh and Sengupta Anirban. 2012. Designing a Filter Bank and an Adaptative Filtering Technique to Eliminate Noises in Power Line Communication. IEEE.

[21] Mlynek Petr, Misurec Siri and Koutny Martin. 2012. Noise Modeling for Power Line Communication Model. IEEE.

[22] Yin Jun, Zhu Xu and Huang Yi. 2014. Modeling of Amplitude-Correlated and Occurrence-Dependent Impulsive Noise for Power Line Communication.

Signal Processing for Communications Symposium. IEEE ICC.

[23] Weyepe J.A., Snyders A.J. and Ferreira H.C. 2012. Implementation of a Gap Recorder for Measuring Impulsive Noise Error Distributions in Power Line Communications Using the Fritzhmana Model. IEEE International Symposium on Power Line Communications and its Applcations.

[24] Middleton David. 1979. Procedures for determining the parameters of the first-order canonical models of class A and class B electromagnetic interference. IEEE Transaction on electromagnetic compatibility. EMC-21: 190.

[25] TEXAS University, UT Austin interference modeling and mitigation. Toolbox 2015.

[26] Degardin V, Lienard M, Zeddam A. 2002. Classification and characterization of impulsive noise on indoor powerline used for data communications. Transactions on Consumer Electronics. 48(4).

[27] Cortés J., Sanz A, Estopiñan P and García J. 2016. On the Suitability of the Midlenton Class A Noise Model for Narrowband PLC. International Symposium on Power Line Communications and its Applications (ISPLC).

[28] Jin L, Li Y, Li B, Wei Z and Shi J. 2015. Performance of Polar Coding for the Power Line Communications in the Presence of Impulsive Noise. IET journals.

[29] Shongwe T, Vinck H and Ferreira H. 2006. On impulse noise and its models. University of Johannesburg, South Africa.

[30] Kim Y, Bae J.N. and Kim J.Y. 2011. Performance of Power Line Communication Systems with Noise Reduction Scheme for Smart Grid Applications. IEEE Trans, Consum.Electron. 57(1): 46-52.

[31] Al-Naffouri T.Y, Quadeer A.A., Al-Shaalon F.F. and Hmida H. 2011. Impulsive Noise Estimation and Cancellation in DSL Using Comprensive Sampling. IEEE ISCAS.

[32] P. a C. Lopes and J. a B. Gerald. 2016. Improving bit error rate under burst noise in OFDM power line communications. Digit. Signal Process. A Rev. J. 51: 47-53.

[33] Gaëtan Ndo, Fabrice Labeau and Marthe Kassouf. 2013. A Markov Middleton model for bursty impulsive noise in modeling and receiver design. IEEE Transactions on Power Delivery. 28(4).

[34] Tran Trung H, Do Dung D and Huynh Tue H. 2013. PLC Impulsive Noise in Industrial Zone: Measurement and Characterization. International Journal of Computer and Electrical Engineering. 5(1).

[35] Güzelgöz Sabih, Celebi Hasan, Güzel Tayyar, Arslan Hüseyin and Mihcak Kivanc. 2010. Time Frecuency Analysis of Noise Generated by Electrical Loads in PLC. 17th International Conference on Telelcomminucations.

[36] F. J. Cañete. 2005. Caracterización y Modelado de Redes Eléctricas Interiores como Medio de Transmisión de Banda Ancha. p. 245.

[37] C. Victor and N. Mtonyole. 2014. Design of Multicarrier Broadband Power Line Communication System for Tanzania Homes. Int. J. Comput. Appl. 100(14): 25-32.

[38] J. Anatory, N. Theethayi, R. Thottappillil and N. H. Mvungi. 2009. A broadband power-line communication system design scheme for typical tanzanian low-voltage network. IEEE Trans. Power Deliv. 24(3): 1218-1224.